The Influence of Direct Non-Thermal Plasma Treatment on Soot Characteristics under Low Exhaust Gas Temperature

Teerapong Iamcheerangkoon[1,4], *Nuwong* Chollacoop[2], *Boonlue* Sawatmongkhon[1,4], *Thawatchai* Wongchang[3,4], *Kampanart* Theinnoi[1,4,*] and *Ekachai* Juntasaro[5]

[1] Department of Power Engineering Technology, College of Industrial Technology, King Mongkut's University of Technology North Bangkok., Thailand
[2] Renewable Energy and Energy Efficiency Research Team, National Energy Technology Center (ENTEC), National Science and Technology Development Agency
[3] Department of Mechanical and Automotive Engineering Technology, Faculty of Engineering and Technology, King Mongkut's University of Technology North Bangkok (Rayong Campus), Rayong, Thailand.
[4] Research Centre for Combustion Technology and Alternative Energy (CTAE), Science and Technology Research Institute, King Mongkut's University of Technology North Bangkok, Thailand
[5] The Sirindhorn International Thai-German Graduate School of Engineering (TGGS), King Mongkut's University of Technology North Bangkok, 1518 Pracharat 1 Road, Wongsawang, Bangsue, Bangkok 10800, Thailand.

Abstract. This study aimed to assess the effectiveness of nonthermal plasma (NTP) technology utilizing a dielectric barrier discharge (DBD) reactor, both with and without exhaust gas recirculation (EGR), in reducing soot particles and their impact on nitrogen oxides (NO_x). The experiment involved maintaining a constant flue gas flow rate of 10 l/min, employing high voltage values of 0, 6, and 10 kV, fixed frequency of 500 Hz and setting the various IMEP of 5, 6, and 7 bar and the engine speed at 2,000 rpm. The findings demonstrated that NTP was successful in removing NO_x by approximately 16.84% and 17.01%, achieving particle matter (PM) removal efficiencies of around 60.79% and 81.13%, and effectively reducing activation energy by approximately 18.34% and 31.5% (with and without EGR, respectively) at a high voltage of 10 kV. These results highlight the potential of NTP technology in mitigating emissions and reducing the environmental impact associated with diesel engines.

Keyword. Diesel engine, EGR, Nonthermal plasma, Soot

1 Introduction

Diesel engines are more efficient than gasoline engines in terms of torque, stability, and fuel economy. However, the primary pollutants of diesel exhaust gas emissions are nitrogen oxides (NO_x) (NO_x is the sum of nitrogen monoxide; NO and nitrogen dioxide; NO_2) and particulate matter (PM), which seriously impact public health. Because PM exposure has been associated with respiratory and cardiovascular conditions [1,2]. This issue is to meet these more stringent standard requirements. Therefore, many research and technological developments in advanced diesel engines have been concerned and developed high-performance after-treatment systems.

The primary PM emission from diesel engines is carbon black. The accumulation mode encompasses the predominant distribution of particle size and particle mass, with concentrations between 10 nm to 30 µm [3]. The particles in this mode exhibit diverse shapes, including individual particles, long chains, or aggregated masses of larger particles [4]. The specific shape of a particle is two parameters according to its generation time and the range of sizes it falls into [3,4]. Describes the particle size division into the following modes: Nucleation mode (5–50 nm); this mode often consists of volatile organic compounds (VOCs), sulphur compounds, and solid carbon that develop during exhaust dilution and cooling. More than 90% of the particle number and 1–20% of the particle mass are frequently found in the nucleation mode. Accumulation mode (50–500 nm); consists of particles in accumulation mode that have been restrained after being deposited on the surfaces of the cylinder and exhaust system, and coarse mode (above 500 nm); the particle mass in the coarse mode ranges from 5–20% [5].

Diesel particulate filters (DPF) are widely acknowledged as the most effective method to reduce PM emissions. Its capture efficiency is more than 95% [6,7], which has become the usual arrangement for post-treatment systems. The DPF has a honeycomb structure consisting of an open square at one end of the DPF, thus forcing the engine exhaust gases through the porous wall of the DPF, causing the PM particles to be filtered through a porous wall. The filtered exhaust gas, without PM, then flows out of the DPF from the outlet channel. However, the mechanism of diffuse deposition, flow interception, inertial collision, and gravity precipitation was used to explain PM accumulation on the surface and inside of

* Corresponding author: kampanart.t@cit.kmutnb.ac.th

porous walls [2]; In this process, the continuously accumulated PM blocks in inlet channels of the DPF, which increased back pressure and fuel consumption, decreased engine performance compared to the regular engine operation.

Therefore, it is necessary to rapidly remove PM from the channel to regenerate the DPF [8]. The most often used active regeneration technique method increasing the exhaust temperature up to 550 ºC [9], by injecting fuel upstream of the Diesel Oxidation Catalyst (DOC), electric heating, microwave heating, etc. [10]; thus oxidizing soot with oxygen (O_2) in a DPF [2]. However, excessive soot loading or fuel injection might result in high temperatures and uncontrolled regeneration from surface oxidation of PM, causing different thermal expansion cracks or melting of the porous supports may occur, causing irreparable damage [7].

The exhaust gas recirculated (EGR), and these exhaust gas and soot particles were once more oxidised inside the cylinder. After using EGR, the Air/Fuel (A/F) ratio decreases [3,11]. Consequently, the oxidation process of polycyclic aromatic precursors and other chemical compounds becomes incomplete when EGR is utilized, increasing the density of primary nuclear-modal particulate matter. Meanwhile, the combustion process also generates active free radicals and intermediate by-products of small molecule combustion, which enter the cylinder with hydrocarbons and aromatic hydrocarbons in the exhaust gas [12]. EGR efficiently reduces NO_x emissions from diesel engines by decreasing cylinder oxygen concentration along with the flame temperature [11,13]. Furthermore, the addition of EGR increased particulate matter emissions [14].

Plasma is the fourth state of matter [15,16], usually combining electrons, ions, and excited and neutral species. An amount of ionic and excited species in plasma with sufficient energy to collide and break the stable molecular structure of the particles passing through it [17]. However, in the nonthermal plasma system, which occurs when the kinetic energy of electrons or temperature is higher than the kinetic energy of gas molecules outside (around ambient temperature) [18-20], electrical energy is transmitted to the electrons, causing the production of free radicals such as N, O, HO_2, and OH [21]. Due to this characteristic, nonthermal plasma (NTP) has a high energy efficiency [22]. Dielectric barrier discharge (DBD) operates between two electrodes. A dielectric layer is present over at least one electrode to prevent spark discharge [23]. In which the dielectric layer restricts the intensity of current accessing the system and distributes the discharge approximately across the entirety of the electrode surface, DBD production typically employs high voltage alternating current (AC), with a typical frequency of 0.05 to 60 kHz [16]. Okubo *et al*., conducted a study on ozone generation from the air using a DBD-NTP reactor [24]. It was found that this promotes NO to NO_2 for improving DPF regeneration at low oxidation temperatures to the soot reduction mechanism proposed by O, OH, O_3 and NO_2 [25,26]. According to Xu (2001), DBD can offer the optimum energy electrons (1 - 10 eV) with a high density to produce low-excited atomic and molecular species, free radicals, and excimers [27].

As a result of the problems encountered above, this research aimed to investigate soot composition from NTP treatment with and without EGR under low exhaust temperature conditions in diesel engines to develop alternative strategies for removing particulate matter.

2 Experimental Setup

2.1 Engine Specifications

A schematic diagram of the experimental design is shown in Figure 1 The diesel engine was used for generating actual exhaust emissions in this research. This experimental study used a common-rail direct injection (DI) diesel engine to meet the Euro Stage V emissions standards specified in Table 1 to simulate the engine load. The engine was connected to an eddy current dynamometer test stand (AVL; EMCON 400). The crankshaft angle and engine speed (rpm) were measured by a high-resolution crankshaft encoder (model 2614C) with a resolution of 0.1 crank angle (CA). Additionally, a pressure transducer (Kitsler; model 6052b1) was mounted inside the cylinder head for real-time analysis of combustion parameters. The Kitsler system (KiBox® To Go; model 2893A121) was used to calculate engine efficiency and measure cylinder pressure. The engine speed was set at a constant of 2,000 rpm, while the Indicated Mean Effective Pressures (IMEP) were compared at 5, 6, and 7 bar (corresponding to 16.3, 25.2, and 32.6 Nm, respectively).

The back pressure valve maintained constant exhaust gas under all conditions. to confirm that other factors did not influence the number, mass, and volume. In conditions without EGR, it was fitted with a flange on the inlet pipe at the EGR valve to prevent the swirling of exhaust gas into the air intake system. All testing conditions were sampled accordingly. A 10 litres per min vacuum pump then transported the exhaust gases to the DBD-NTP treatment system; engine exhaust emissions were analysed using an exhaust gas analyser (TESTO; model 350) and particle size and quantity were measured by Engine Exhaust Particle Spectrometer (EEPS; model TSI 3090).

Table 1. Engine specifications.

Models	Common rail diesel engine Euro Stage V
Displacement volume	2499 cm^3
Combustion system	Direct injection
Bore	95.4 mm.
Stroke	87.4 mm.
Maximum torque	280 N.m. at 1,800 – 2,200 rpm
Maximum power	8.7 kW at 1,800 – 2,200 rpm

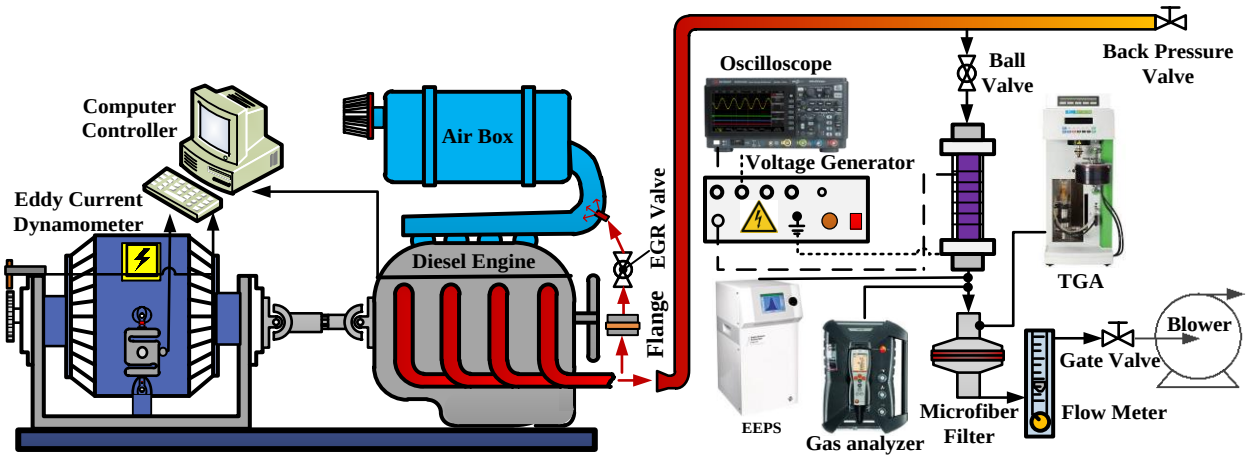

Fig. 1. Schematic diagram of the experimental design.

2.2 Nonthermal Plasma Setup

The dielectric barrier discharge (DBD) for nonthermal plasma (NTP) reactor consists of a metal rod as a high-voltage electrode core with a diameter of 10 mm and a quartz glass tube as a dielectric barrier discharge with an inner diameter of 17 mm. The discharge gap was set at a constant of 3.5 mm. The ground electrode was a stainless steel tube, and the effective discharge length (was 100 mm). The alternating current (AC) voltage in the DBD-NTP system is adjustable at 6 kV (1.152 watts) and 10kV (3.2 watts) with an Oscilloscope (KEYSIGHT; model DSOX 1204G) to determine the voltage of an alternating current (AC), were sent to amplify the High Voltages Power Supply: HVPS (TREK; model 10/10B-HS) with a voltage gain ratio of (1:1,000 voltage and 1 V/4 mA) and constant frequency fixed at 500 Hz according to all conditions. The transformer used in the experiment contains a conversion ratio of 1 V input to 4 mA output, which is used to determine the current. The voltage was the conversion ratio of Voltage (peak to peak) input per 1:1,000 V output.

The DBD-NTP system's exhaust flow rate is then controlled at 10 litres per min after some engine exhaust gases are drawn from the vacuum pump and treated before being released back into the gas treatment system again. Maintain the exhaust gas components in a gaseous condition in the exhaust gas derived from the diesel engine's combustion. The DBD-NTP system is temperature controlled to match the engine exhaust gas temperature. The heating tape was installed in the piping system before the DBD-NTP reactor and microfiber filter sampling; this prevents condensation in the exhaust system and results in more efficient control of the voltage supply at the DBD-NTP reactor.

2.3 Thermogravimetric analysis (TGA)

In analysing different components of combustion-related soot, the soot is captured by glass microfiber filter papers (Whatman Grade GF/C with 1.2µm pore size). The results were analysed by a Thermogravimetric Analyzer (TGA; PerkinElmer model Pyris1), which can identify the composition of soot particles, moisture (H_2O), VOCs and carbon (Element Carbon) [9,21] obtained from the microfiber filter. Table 2 contains a list of the TGA heating programme. The procedure was created to estimate the concentrations of H_2O, VOCs, and carbon soot at established weight loss temperatures [28].

Table 2. TGA temperature program.

Step	Temperature Program	Period (min)	Atmosphere
1	Isothermal at 40 ℃	10	N_2 (50 ml/min)
2	Heating to 110 ℃ (10 ℃/min)	7	N_2 (50 ml/min)
3	Isothermal at 110℃	30	N_2 (50 ml/min)
4	Heating to 400 ℃ (10 ℃/min)	29	N_2 (50 ml/min)
5	Isothermal at 400 ℃	30	N_2 (50 ml/min)
6	Cooling to 300 ℃ (10 ℃/min)	10	N_2 (50 ml/min)
7	Heating to 600 ℃ (10 ℃/min)	30	O_2 (50 ml/min)
8	Isothermal at 600 ℃	30	O_2 (50 ml/min)

3 Results and discussion

3.1 The combustion characteristic

Firstly, monitoring the In-cylinder pressure and HRR to describe engine performance of operating conditions is necessary. As shown in Figure 2, the differences between with and without EGR are based on a B7 diesel. Selecting the low load condition, three selected IMEPs were 5, 6 and 7 bar. The combustion parameters were checked as follows based on the cylinder pressure data.

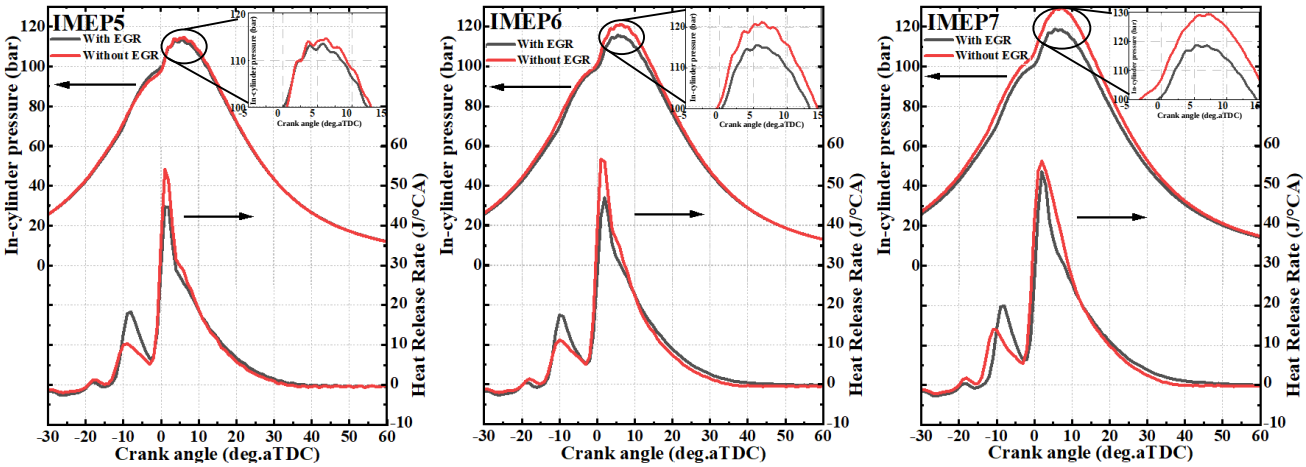

Fig. 2. Comparison graph between the in-cylinder pressure and the heat release rate at IMEP of (Left) 5, (Middle) 6 and (Right) 7 bar under conditions with and without EGR.

It was determined that pilot and primary injections were at -8 °Ca before TDC and 1 °Ca after TDC, respectively. Based on the cylinder pressure measurements, the in-cylinder pressure was somewhat higher at IMEP 5 bar. Nevertheless, it increases at IMEP 6 and 7 bar (4.84% and 8.98%, respectively) [29]. During the main combustion processes (in black line), The engine operated without EGR show higher in-cylinder pressures compare to the engine operating with EGR (in red line) Due to exhaust gas being introduced to the intake manifold [11,13], which reduced oxygen concentration and increased the specific heat capacity of intake, resulting in lower effective fuel/air mixing and worse in-cylinder combustion performance [12]. At the pilot injection, EGR usage was applied in all IMEPs, and the effect of the HRR was increased when compared to that without EGR due to the exhaust gas being recirculated at a higher temperature than intake air [13].

3.2 Exhaust gas emissions

The engine load 6 bar IMEP has been selected for the in-cylinder pressure to analyse the effect of starting to change in the cylinder pressure. Figure 3 illustrates the O_2 concentration in the exhaust gas. It was found that combustion with EGR requires a higher O_2 than without EGR leading to the reduced amount of O_2 used in EGR combustion in a cylinder to keep engine stability [11-14]. On the other hand, when DBD-NTP was activated, the O_2 content was slightly insignificantly altered in both conditions. DBD-NTP results in free electrons reacting with oxygen bonds until breaking down to active oxygen (O*). Then, it interacts with O_2 to produce O_3, as demonstrated in equations (3) and (8).

Figure 4 illustrates the impact of DBD-NTP on NO and NO_2 between conditions with and without EGR. It was found that in the conditions where EGR was applied, a significant (71.78 %) reduction in NO_x content was observed as a result of EGR, which contributes to NO_x reduction [11,13]. Under EGR conditions, there is a slight increase in NO_2 at a voltage of 6 kV (3.31 %). On the other hand, at a voltage of 10 kV, the amount of NO_2 increases by 5.99%. However, the amount of NO decreases by 100%, which is in the same direction as in non-EGR conditions, when increasing the voltage to 10 kV, due to the voltage can transmit energy to electrons, causing free radicals [21,22] from the amount of NO_2 that increases significantly by 59.3%. Moreover, the total NO_x has reduced by approximately 16.84% and 17.01% (with and without EGR, respectively) at a high voltage of 10 kV. [16, 30-33] describes the reactions of DBD-NTP to NO_x removal, dividing them into two main groups.

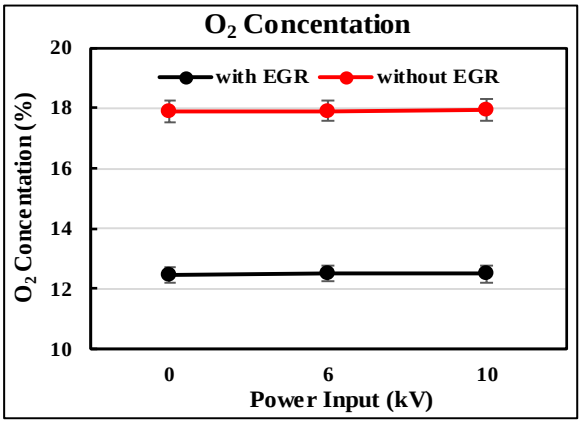

Fig. 3. Effect of DBD-NTP on O_2 concentration under conditions with and without EGR.

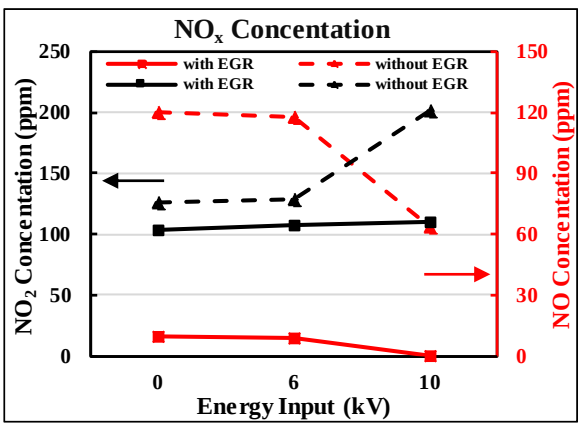

Fig. 4. Effect of DBD-NTP on NO and NO_2 concentration under engine operated with and without EGR.

The first group, the primary and principal of NO_x elimination reactions may be found in Equations (1) - (7):

$$N_2 + e^* \rightarrow N + N + e \quad (1)$$

$$NO + N \rightarrow N_2 + O \quad (2)$$

$$O_2 + O^* \rightarrow O_3 \quad (3)$$

$$N_2 + e \rightarrow e + N_2\,(A) \quad (4)$$

$$N_2\,(A) + NO \rightarrow N_2 + N + O \quad (5)$$

$$N_2\,(A) + N_2O \rightarrow 2N_2 + O \quad (6)$$

$$NO_2 + N \rightarrow N_2 + O_2 \quad (7)$$

where N_2 (A) represents the N_2 metastable state.

Equations (8) - (10) provide a summary of the second group of processes (which includes the reactions oxidising NO to NO_2):

$$O_2 + e^* \rightarrow O^* + O^* + e \quad (8)$$

$$NO + O^* \rightarrow NO_2 \quad (9)$$

$$NO + O_3 \rightarrow NO_2 + O_2 \quad (10)$$

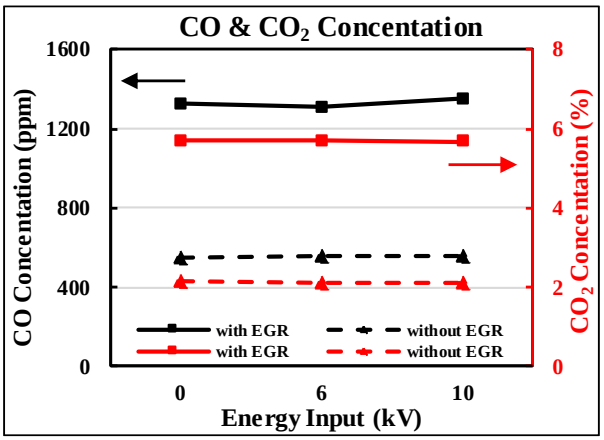

Fig. 5. Effect of DBD-NTP on CO and CO_2 concentration under conditions with and without EGR.

Figure 5 illustrates the effect of DBD-NTP on CO and CO_2 concentrations. The use of EGR increases CO and CO_2 by approximately 58.2% and 62.98%, respectively, when compared with the inactivity of EGR. The CO_2 concentration in the exhaust gas is slightly reduced by 0.13% and 2.67% (with and without EGR, respectively) at a high voltage of 10 kV. The CO concentration has a small and insignificant change in the same direction. The electrical field can be sufficiently strong to excite carbon dioxide molecules due to the more significant electric field and discharge power, which provide electrons more energy to begin their impact reactions [18,34]. Equations (11) - (15) describe regular reaction processes for breaking down CO_2 molecules in plasma [18].

$$CO_2 + O \rightarrow CO + O_2 \quad (11)$$

$$CO_2 + O_2 \rightarrow CO + O_3 \quad (12)$$

$$e + CO_2 \rightarrow CO + O + e \quad (13)$$

$$e + CO^*_2 \rightarrow CO + O \quad (14)$$

$$2CO_2 + 2N^*_2 \rightarrow 2CO + O_2 + 2N_2 \quad (15)$$

The equations (16) can reduce CO_2 concentration by including electron impact reactions and multiple active oxygen species: Where CO_2 and N_2 are, respectively, the excited types of the CO_2 and N_2 molecules, and CO generated through various processes have different amounts of energy [15].

$$C + O_3 \rightarrow CO + O_2 \quad (16)$$

On the other hand, the DBD-NTP system reacts with CO and active oxygen as in equations 17-18, which is a reverse entanglement reaction. As a result, the amount of CO and CO_2 was slightly converted [35].

$$CO + O \rightarrow CO_2 \quad (17)$$

$$CO + O_3 \rightarrow CO_2 + O_2 \quad (18)$$

3.3 Particulate size distribution and Soot compositions

Effect of DBD-NTP with different power inputs on the particle size distribution of PM under with and without EGR conditions. As shown in Figure 6a), PM showed that the particle size distribution was mainly concentrated in the areas between 22.5 - 165 nm and 7 - 45 nm with and without EGR application, respectively. When the engine load increases, the particle quantitative concentration curve's peak value and size gradually increase.

Under the EGR applied condition, it was found that most of the particle size distributions were concentrated in the region between 22.1 - 165.5 nm. In the presence of DBD-NTP at 6 kV, the particle content was reduced by 37.41% (at IMEP 6 bar) from when particles flowing through the DBD-NTP reaction phase have free electrons colliding [27], causing PM particles to split to a small size. The voltage was increased by 10 kV, the PM particle content effectively decreased by 57.49% (at IMEP 6 bar), and PM particles were increased in the particle size distribution range of 8.06 - 22.1 nm. However, the plasma treatment was an increase in the ultrafine particulate matter (8.06 - 22.1 nm). The energy being delivered is sufficient to break up large particles into smaller particles. These phenomena could be clarified by the fact that the plasma zone was produced by the discharge of large-scale particles, which were classified as accumulating and primarily composed of electrically conductive carbon spheres [3]. This indicates that the decrease in large-size particles was effective [9]. In addition, when EGR is disabled shows multi-peak distribution remaining within the nucleation mode range. The highest peak is in the range of 6.98 - 14.3 nm and the second peak is in the range of 14.3 - 45.3 nm. This is primarily caused by the cylinder's decreased oxygen concentration in the application of EGR, which promotes the mass synthesis of carbon core particles and, consequently, increases the number of nuclear mode particles [3]. However, the appearance of NTP can reduce the particulate number

distribution by 4.86% (6kV) and 55.81% (10kV) as shown in Figure 6a.

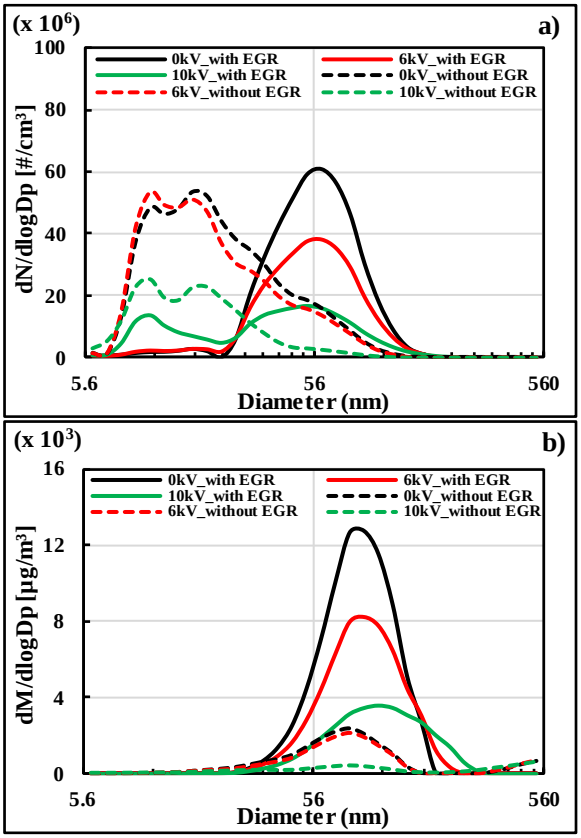

Fig. 6. Effect of DBD-NTP on the a) particulate number distribution and b) particulate mass distribution under conditions with and without EGR.

The relation between particle mass and particulate number, as shown in Figure 6b, is attributed to the fact that particulates in the accumulation mode contribute significantly to the particle mass. Although Kittelson's suggests that particles in the nuclei mode account for more than 90% of the total particle number [36], the data collected indicates that particles in the nuclei mode exhibit a relatively low particle number. Moreover, the observed increase in ultrafine particulate matter (as shown in Figure 6a) has a minimal influence on the mass distribution due to the slight increase in the ultrafine particulate matter mass compared to the mass distribution represented by dN [9]. In the EGR-active condition, the presence of DBD-NTP resulted in a reduction in particle mass of 37.02% and 60.79% at power inputs of 6 and 10 kV, respectively. These findings are consistent with the conditions without EGR, where the particle mass decreased by 9.92% and 81.13% at power inputs of 6 and 10 kV, respectively. These results indicate that DBD-NTP is effective in reducing particulate mass.

Figure 7 shows the results of the analysis conducted with EGR; Figure 7a) illustrates the weight loss penetration of soot oxidation, while Figure 7b demonstrates the derivative weight loss of soot oxidation. The derivative weight loss outcomes obtained from utilising DBD-NTP at 0,6 and 10 kV demonstrate an expected peak at approximately 500 - 550 °C, indicating the presence of the same carbon type in the soot composition. The derivative weight loss result from TGA analysis provides information about the slope of the TGA spectra, which reflects the activity of soot oxidation and its impact on the activation energy of soot combustion. The amplitude of derivative weight loss follows the order of 0 kV > 6 kV > 10 kV, indicating the activation energy of soot combustion.

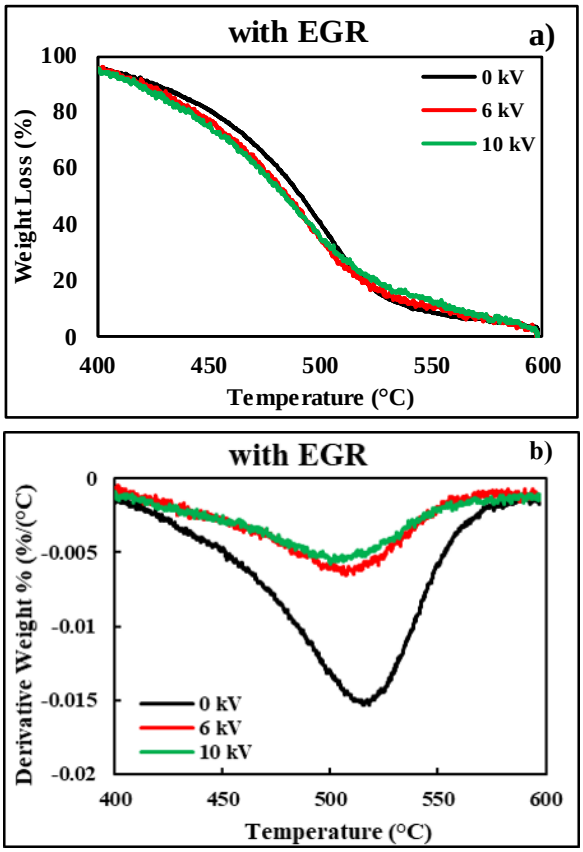

Fig. 7. Effect of DBD-NTP a) weight loss and b) Derivative weight on temperature with EGR conditions.

In this case, the analysis was performed without EGR, and the obtained results are presented in Figure 8. The weight loss penetration of soot oxidation, while the derivative weight loss of soot oxidation was shown in Figure 8b. The results agreed with those obtained when DBD-NTP was paired with EGR, showing the same carbon in the soot composition, as demonstrated by the derivative peak at 500 - 550 °C. The exact order of amplitude of derivative weight loss was observed in the case without EGR. The results obtained from the analysis conducted without EGR agreed with those obtained with EGR, demonstrating the presence of the same type of carbon in the soot composition.

3.4 Activation Energy (Ea)

The activation energy (Ea) analysis is a crucial method to investigate the oxidation kinetics of soot samples. The value of Ea determines the energy required to initiate the oxidation process of elemental carbon. A lower value of Ea indicates that less energy is needed to start the

oxidation process, resulting in faster oxidation kinetics. The Arrhenius equation calculates the value of Ea, which describes the relationship between the rate of a chemical reaction and the temperature at which it occurs. The activation energy of soot samples obtained from raw and DBD-NTP exhaust was analyzed by constructing scatter plots of Ln(-dm/dt) against 1/T, as shown in Figure 9. To ensure the accuracy and reliability of the findings, linear regression analysis was conducted, with correlation coefficients (R^2) exceeding 0.85. The plot's fitted straight-line slope corresponded to the activation energy.

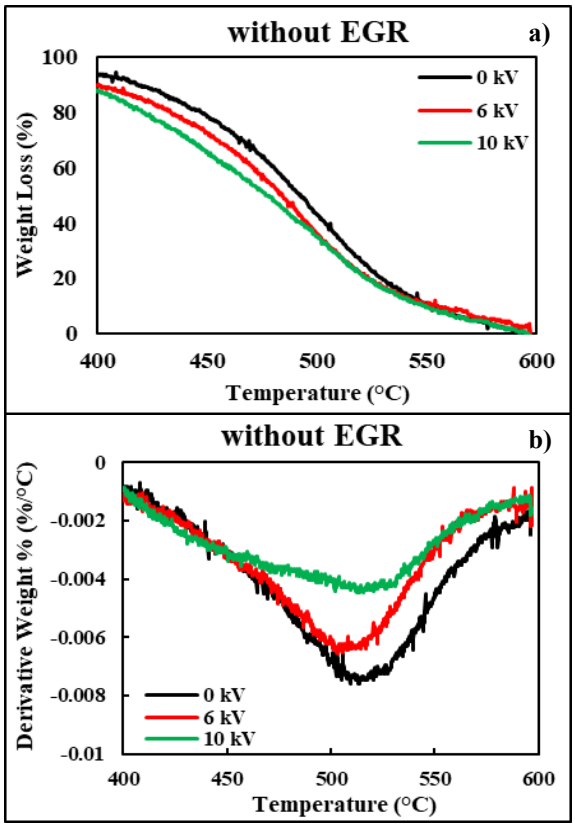

Fig. 8. Effect of DBD-NTP a) weight loss and b) Derivative weight on temperature without EGR conditions.

Figure 10 compares the Ea between the cases of DBD-NTP combined with and without EGR, utilizing energy inputs of 0, 6, and 10 kV. In the DBD-NTP combination with EGR, an increase in energy input leads to a decrease in Ea. Specifically, the Ea at 6 kV is reduced by 7.83% compared to that at 0 kV. Similarly, in the case of 10 kV, the Ea is reduced by 18.34% compared to 0 kV. These findings indicate that higher energy inputs in the DBD-NTP EGR configuration result in lower activation energy values, suggesting enhanced oxidation kinetics and improved effectiveness in soot removal.

In the DBD-NTP without EGR, it has been observed that an increase in energy input results in a decrease in Ea. More precisely, at an energy input of 6 kV, the Ea is found to be reduced by 18.66% compared to its value at 0 kV. Similarly, at an energy input of 10 kV, the Ea is reduced by 31.5% compared to its value at 0 kV. These findings suggest that increasing the energy input can lead to a more efficient and effective DBD-NTP process, enabling the development of novel applications in various fields. However, a comparison between DBD-NTP was combined with and without EGR reveals distinct activation energy (Ea) values. The case of DBD-NTP without EGR demonstrates lower Ea values than DBD-NTP combined with EGR. These findings indicate that utilizing DBD-NTP alone exhibits a higher degree of soot oxidation promotion than when DBD-NTP is combined with EGR.

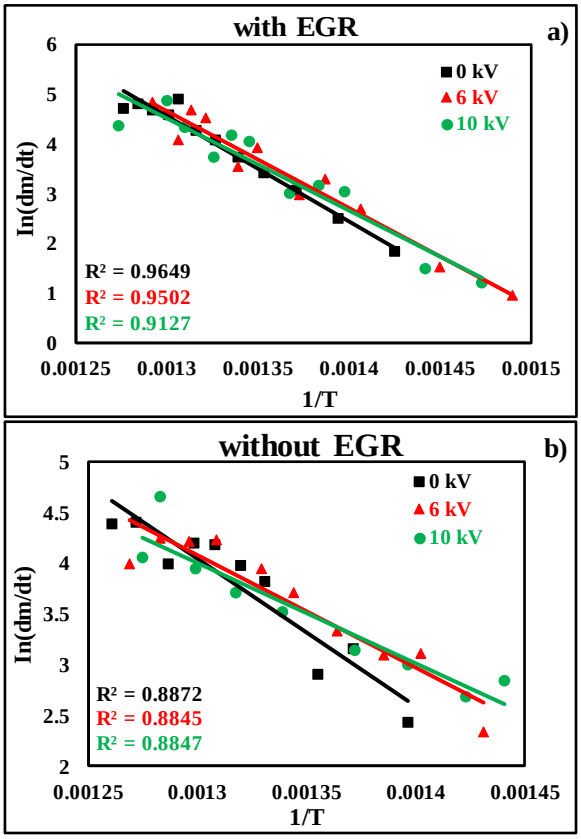

Fig. 9. The Arrhenius equation plots, a) with EGR and b) without EGR

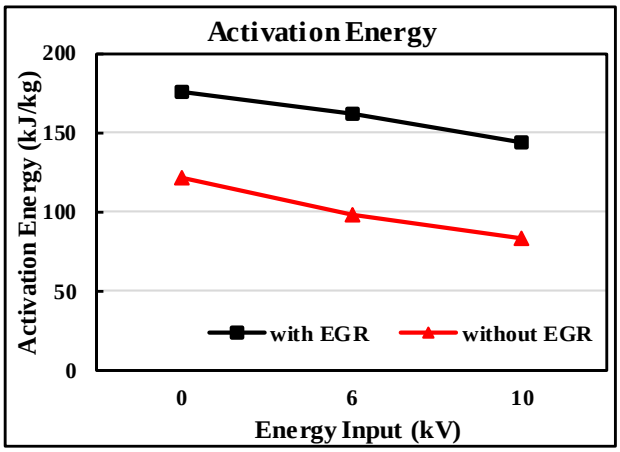

Fig. 10. Effect of DBD-NTP to Activation Energy on the power input under conditions with and without EGR.

4 Conclusion

This research investigates the composition of soot generated by NTP treatment in diesel engines, specifically focusing on examining the impact of EGR under low exhaust temperature conditions. The aim is to explore alternative methods for effectively reducing PM emissions. The DBD-NTP technique and EGR are conducted using a DBD reactor in the real diesel exhaust gas while the effects of EGR are evaluated. The results indicate that DBD-NTP treatment reduces NO_x by approximately 16.84% and 17.01% when using EGR and without EGR, respectively. Additionally, the experiments demonstrate the generation of significant free radicals due to efficient energy transmission from high voltage. Moreover, NTP treatment exhibits effective removal of PM, with removal efficiencies of approximately 60.79% and 81.13% (with and without EGR, respectively). Increasing the voltage level leads to a continuous reduction in PM concentration. NTP treatment also enhances the oxidative activity of PM and reduces the activation energy required for PM dispersion by 18.34% (with EGR) and 31.5% (without EGR) at a high voltage of 10 kV. These findings underscore the promising potential of NTP technology in reducing emissions and improving the environmental impact of diesel engines.

Acknowledgements

This research was funded by the National Science, Research, and Innovation Fund (NSRF), and King Mongkut's University of Technology, North Bangkok, with Contract no. KMUTNB-FF-66-19. T. Iamcheerangkoon thanks King Mongkut's University of Technology, North Bangkok, and the National Science and Technology Development Agency, Thailand. Contract No. Grad 017/2563, for supporting his scholarship.

References

1. K.S. Martirosyan, K. Chen, D. Luss, Behavior features of soot combustion in diesel particulate filter, Chemical Engineering Science, **65**,1 (2010): 42-46
2. S.S. Gill, G.S. Chatha, A. Tsolakis, Analysis of reformed EGR on the performance of a diesel particulate filter, International Journal of Hydrogen Energy, **36**,16 (2011): 10089-10099
3. Z. Wang, X. Zhang, J. Guo, C. Hao, Y. Feng, Particle emissions from a marine diesel engine burning two kinds of sulphur diesel oils with an EGR & scrubber system :Size, number & mass, Process Safety and Environmental Protection, **163** (2022): 94-104
4. N. Ladommatos, S.M. Abdelhalim, H. Zhao, Z. Hu, The dilution, chemical, and thermal effects of exhaust gas recirculation on diesel engine emissions-Part 4: effects of carbon dioxide and water vapour, SAE transactions, (1997): 1844-1862
5. D.B. Kittelson, Engines and nanoparticles: a review, Journal of aerosol science, **29**,5-6 (1998): 575-588
6. Z. Meng, J. Li, J. Fang, J. Tan, Y. Qin, Y. Jiang, Z. Qin, W. Bai, K. Liang, Experimental study on regeneration performance and particle emission characteristics of DPF with different inlet transition section lengths, Fuel, **262** (2020): 116487
7. Y. Shi, Y. Lu, Y. Cai, Y. He, Y. Zhou, J. Fang, Evolution of particulate matter deposited in the DPF channel during low-temperature regeneration by non-thermal plasma, Fuel, **318** (2022): 123552
8. S. Choi, K.C. Oh, C.B. Lee, The effects of filter porosity and flow conditions on soot deposition/oxidation and pressure drop in particulate filters, Energy, **77** (2014): 327-337
9. T. Iamcheerangkoon, N. Chollacoop, B. Sawatmongkhon, T. Wongchang, S. Sittichompoo, S. Chuepeng, K. Theinnoi, Promotion of the NO-to-NO2 conversion of a biofueled diesel engine with nonthermal plasma-assisted low-temperature soot incineration of a diesel particulate filter, Energies, **15**,24 (2022): 9330
10. J. Rodríguez-Fernández, J.J. Hernández, J. Sánchez-Valdepeñas, Effect of oxygenated and paraffinic alternative diesel fuels on soot reactivity and implications on DPF regeneration, Fuel, **185** (2016): 460-467
11. A. Jain, A.P. Singh, A.K. Agarwal, Effect of split fuel injection and EGR on NOx and PM emission reduction in a low temperature combustion (LTC) mode diesel engine, Energy, **122** (2017): 249-264
12. B. Zhao, X. Liang, K. Wang, X. Lv, Y. Wang, Soot particles undergo in-cylinder oxidation again via EGR recirculated gas: Analysis of exhaust soot particle characteristics, Journal of Aerosol Science, **172** (2023): 106190
13. M.M. Abdelaal, A.H. Hegab, Combustion and emission characteristics of a natural gas-fueled diesel engine with EGR, Energy conversion and management, **64** (2012): 301-312
14. A. Abu-Jrai, A. Tsolakis, K. Theinnoi, R. Cracknell, A. Megaritis, M.L. Wyszynski, S.E. Golunski, Effect of gas-to-liquid diesel fuels on combustion characteristics, engine emissions, and exhaust gas fuel reforming, Comparative study, Energy & fuels, **20**,6 (2006): 2377-2384
15. M. Keidar, I. Beilis, Plasma engineering: applications from aerospace to bio and nanotechnology, Academic Press, (2013): 3-100
16. P. Talebizadeh, M. Babaie, R. Brown, H. Rahimzadeh, Z. Ristovski, M. Arai, The role of non-thermal plasma technique in NOx treatment: A review, Renewable and Sustainable Energy Reviews, **40** (2014): 886-901
17. S. Meng, W. Li, Z. Li, H. Song, Non-thermal plasma assisted catalytic thiophene removal from fuel under different atmospheres, Journal of Cleaner Production, **369** (2022): 133282
18. M. Babaie, P. Davari, P. Talebizadeh, F. Zare, H. Rahimzadeh, Z. Ristovski, R. Brown, Performance

evaluation of non-thermal plasma on particulate matter, ozone and CO2 correlation for diesel exhaust emission reduction, Chemical Engineering Journal, **276** (2015): 240-248

19. S. Mohapatro, N.K. Sharma, A. Madhukar, Abatement of NOX using compact high voltage pulse power supply: Towards retrofitting to automobile vehicle, IEEE Transactions on Dielectrics and Electrical Insulation, **24**,5 (2017): 2738-2745
20. A. Fridman, A. Chirokov, A. Gutsol, Non-thermal atmospheric pressure discharges, Journal of Physics D: Applied Physics, **38**,2 (2005): R1
21. T. Wongchang, S. Sittichompoo, K. Theinnoi, B. Sawatmongkhon, S. Jugjai, Impact of high-voltage discharge after-treatment technology on diesel engine particulate matter composition and gaseous emissions, ACS omega, **6**,32 (2021): 21181-21192
22. B. Huang, C. Zhang, H. Bai, S. Zhang, K.K. Ostrikov, T. Shao, Energy pooling mechanism for catalyst-free methane activation in nanosecond pulsed non-thermal plasmas, Chemical Engineering Journal, **396** (2020): 125185
23. S. Yao, Plasma reactors for diesel particulate matter removal, Recent patents on chemical engineering, **2**,1 (2009): 67-75
24. M. Okubo, N. Arita, T. Kuroki, T. Yamamoto, Total diesel emission control system using ozone injection and plasma desorption, In Fourtieth IAS Annual Meeting. Conference Record of the 2005 Industry Applications Conference, **4** (2005): 2924-2931
25. P. Wang, W. Gu, L. Lei, Y. Cai, Z. Li, Micro-structural and components evolution mechanism of particular matter from diesel engines with non-thermal plasma technology, Applied thermal engineering, **91** (2015): 1-10
26. M. Okubo, T. Kuroki, S. Kawasaki, K. Yoshida, T. Yamamoto, Continuous regeneration of ceramic particulate filter in stationary diesel engine by nonthermal-plasma-induced ozone injection, IEEE Transactions on Industry Applications, **45**,5 (2009): 1568-1574
27. X. Xu, Dielectric barrier discharge-properties and applications, Thin solid films, **390**,1-2 (2001): 237-242
28. J. Rodríguez-Fernández, F. Oliva, R.A. Vázquez, Characterization of the diesel soot oxidation process through an optimized thermogravimetric method, Energy & Fuels, **25**,5 (2011): 2039-2048
29. M. Elkelawy, E.A. El Shenawy, S.A. Mohamed, M.M. Elarabi, H.A.E. Bastawissi, Impacts of EGR on RCCI engines management: A comprehensive review, Energy Conversion and Management: X, **14** (2022): 100216
30. Y. Miao, A. Yokochi, G. Jovanovic, S. Zhang, A. von Jouanne, Application-oriented non-thermal plasma in chemical reaction engineering: A review, Green Energy and Resources, (2023): 100004
31. T. Aka-Ngnui, A. Beroual, Non-thermal plasmas for NOx treatment, In IMETI, (2009): sur-CD
32. G.B. Zhao, X. Hu, M.C. Yeung, O.A. Plumb, M. Radosz, Nonthermal Plasma Reactions of Dilute Nitrogen Oxide Mixtures: NO x in Nitrogen, Industrial & engineering chemistry research, **43**,10 (2004): 2315-2323
33. G. Sathiamoorthy, S. Kalyana, W.C. Finney, R.J. Clark, B.R. Locke, Chemical reaction kinetics and reactor modeling of NO x removal in a pulsed streamer corona discharge reactor, Industrial & engineering chemistry research, **38**,5 (1999): 1844-1855
34. X. Pu, Y. Cai, Y. Shi, J. Wang, L. Gu, J. Tian, and W. Li, Diesel particulate filter (DPF) regeneration using non-thermal plasma induced by dielectric barrier discharge, Journal of the Energy Institute, **91**,5 (2018): 655-667
35. M.R. Khani, E. Barzideh Pour, S. Rashnoo, X. Tu, B. Ghobadian, B. Shokri, A. Khadem, S.I. Hosseini, Real diesel engine exhaust emission control: indirect non-thermal plasma and comparison to direct plasma for NO x, THC, CO, and CO 2, Journal of Environmental Health Science and Engineering, **18** (2020): 743-754
36. D.B. Kittelson, Engines and nanoparticles: a review, Journal of aerosol science, **29**,5-6 (1998): 575-588